LBL-30364
Preprint

Lawrence Berkeley Laboratory
UNIVERSITY OF CALIFORNIA

Materials & Chemical Sciences Division

Submitted to the Journal of Physical Chemistry

Dynamics of Ba-Br_2 Chemi-Ionization Reactions

A.G. Suits, H. Hou, H.F. Davis, and Y.T. Lee

February 1991

Prepared for the U.S. Department of Energy under Contract Number DE-AC03-76SF00098

DISCLAIMER

DISCLAIMER

LBL-30364

DYNAMICS OF Ba-Br_2 CHEMI-IONIZATION REACTIONS

Arthur G. Suits, Hongtao Hou, H. Floyd Davis,
and Yuan T. Lee

Department of Chemistry
University of California

and

Chemical Sciences Division
Lawrence Berkeley Laboratory
Berkeley, CA 94720 USA

February 1991

This work was supported by the Director, Office of Energy Research, Office of Basic Energy Sciences, Chemical Sciences Division, of the U.S. Department of Energy under Contract No. DE-AC03-76SF00098.

Dynamics of Ba-Br_2 Chemi-ionization Reactions

Abstract

The formation of $BaBr^+$ ions in reaction of $Ba(^1S_0,^1P_1)$ with Br_2 was studied as a function of laboratory scattering angle and product translational energy in a crossed beams experiment. The contour map of $BaBr^+$ flux obtained for the ground state reaction at 1.1 eV collision energy showed a backscattered angular distribution (relative to the barium beam) with a substantial fraction of the available energy appearing in translation. Laser excitation strongly inhibited this channel at 1.1 eV. These experimental observations suggest that for the chemi-ion reaction head-on, collinear collisions and proximal crossings of the potential energy surfaces are necessary to preclude escape into the dominant neutral pathways. At 1.6 eV collision energy a new laser-dependent source of $BaBr^+$ appeared. This laser-enhanced $BaBr^+$ showed a laboratory angular distribution substantially narrower than for the ground state reaction, indicating a smaller translational energy release. The angular distribution was ~70% backscattered and displayed a clear dip at the center of mass. This new $BaBr^+$, produced from electronically excited barium at higher translational energy, is ascribed to secondary collisions of BaBr + Br initially formed in low impact parameter collisions. Reaction of electronically excited barium with Br_2 also yielded an associative ionization product $BaBr_2^+$ at both collision energies studied, with a cross section about 1/100th that of the chemi-ion channel.

I. INTRODUCTION

The reaction of barium with halogen molecules represents an important prototypical case for the study of reaction dynamics in divalent systems.[1-6] Reaction may be initiated with the transfer of one electron via the celebrated "harpoon mechanism",[7-10] but there exist a range of possible product channels owing to the presence of the second valence electron on barium and a second electron-accepting halogen atom. The reaction with ground state barium is dominated by the production of the ground state, neutral radical pair BaX and X (X a halogen atom).[11,12] In addition, there also exist exoergic electronically excited neutral product channels, and a chemi-ion channel: BaX^+ and X^-.[13]

This chemi-ionization reaction corresponds to the transfer of both valence electrons from barium to the halogen molecule. The BaX^+ formation thus provides a window into the dynamics of the second electron transfer. The reaction of ground state barium with chlorine yielding $BaCl^+$ was studied under crossed beam conditions by Ross and co-workers.[14] Their results suggested either backscattering with respect to the effusive barium source, or forward-backward symmetry of the $BaCl^+$ product distribution with respect to the relative velocity vector. They interpreted their results to indicate the importance of a strongly coupled collision for the chemi-ion channel. Recently we reported clearly backscattered angular distributions of $BaCl^+$ from this reaction performed under better defined conditions,[15] confirming the importance of an

intimate Ba-Cl-Cl interaction. This reaction was found to be strongly inhibited by electronic excitation of the barium, consonant with a mechanism in which the nascent BaCl formed as a result of the initial electron transfer must "pursue" the departing chlorine atom in order to reach a portion of the potential energy surface which is crossed by the doubly ionic surface correlating to $BaCl^+$ and Cl^-. Only for low impact parameter, near collinear collisions will this be possible. We here extend these studies to the measurement of translational energy and angular distributions of $BaBr^+$ product flux in an effort to achieve some quantitative understanding in the analogous Ba + Br_2 reaction. In addition, we describe a new laser dependent source of $BaBr^+$ for which no analogue appeared in the Cl_2 studies.

II. EXPERIMENTAL

A supersonic barium beam was formed by expanding mixtures of barium and neon or argon from the nozzle of a resistively heated one-piece molybdenum oven assembly to be described in detail in a forthcoming publication.[16] Under typical operating conditions, the nozzle was ~1500°C, while the barium reservoir was maintained about 300°C cooler. An auxiliary radiative graphite heating element surrounding the barium reservoir allowed its temperature to be adjusted independently of the nozzle temperature. The barium beam passed through a heated molybdenum skimmer and a collimating slit, then to a collision chamber maintained at ~10^{-7} Torr.

The bromine beam was produced by expanding a 3% Br_2/He mixture through a 0.075 mm nozzle heated to 200°C. The bromine beam passed through a skimmer and collimating slit to cross the barium beam at 90° in the collision chamber, yielding a cubic interaction volume of 2^3 mm.

The interaction region of the collision chamber was surrounded by a stainless steel electrode and aperture plate of the detector, shown in Figure 1, floated field-free 120V above ground. Ions produced in the reaction were allowed to scatter in the field-free region. Those which entered the floated aperture attached to the detector were then accelerated to ground potential at the entrance to a quadrupole mass spectrometer through focusing lenses and a retarding electrode. Mass selected ions were counted by means of a Daly type scintillation ion detector and associated electronics.[17] The entire detector assembly could be rotated in the plane of the two beams, allowing for measurement of product flux as a function of laboratory scattering angle. The retarding potential, gating and scalers were controlled by computer: for laser on/off experiments the retarding potential was stepped at 4 Hz along with a laser flag so that simultaneous laser on/off and signal/background could be recorded. For translational energy scans the retarding potential was applied as a 100 mV, 100 Hz square wave riding on a DC voltage, stepped up through the energy range of interest. Data corresponding to the high and low retarding voltage steps were recorded and subtracted to yield the differential energy scans. At the low energy region, signals are often the result of subtraction of two large numbers. The error bars are thus larger at the low energy regions of the spectra. Some minor energy-dependent focusing was

observed when retarding potential was applied. At angles of intense signal, when low energy signal is very small, a small variation in transmission of high energy signal resulting from the applied retarding potential can appear as negative signal in the first few points of the scans. For the experiments reported here, this was sufficiently far from the region where the product signal appeared to cause no interference. In addition, owing to the cylindrical symmetry of the scattering process with respect to the relative velocity vector, we need not rely on product appearing at low laboratory energies to obtain a complete picture of the flux distribution.

Electronically excited barium atoms were prepared by optical pumping at the interaction region by means of a single-frequency ring dye laser tuned to the $Ba(^1S_0$-$^1P_1)$ transition at 553.7 nm. The fluorescence from the $Ba(^1S_0$-$^1P_1)$ transition was directed through a telescope onto a photomultiplier tube and recorded along with the data.

III. RESULTS

A. $Ba(^1S_0) + Br_2$

The crossed beams reaction of ground state barium with Br_2 was studied at a collision energy of 1.1 eV. Translational energy scans for $BaBr^+$ products were obtained with a retarding field energy analyzer at various laboratory scattering angles. These scans are shown in Figure 2 along with fits obtained by forward convolution of assumed forms of the center of mass angular ($T(\Theta)$) and translational energy distributions ($P(E)$), assumed to be independent. The convolution includes angular divergence of the beams and measured spreads of the beam velocities ($v/\delta v$ ~8 and 10 for barium and bromine beams, respectively).

The fits shown in Figure 2 yield the contour map of $BaBr^+$ flux shown superimposed on the nominal Newton diagram in Figure 3. Greater than 80% of the flux appears in the backward direction (forward is considered to be in the direction of the barium beam). This strongly backscattered $BaBr^+$ distribution is even more remarkable when one considers the possible smearing of the angular distribution from the range of initial recoil angles by coulomb attraction of the recoiling ion pair.

The broad translational energy distribution peaks near 0.7 eV, but >30% of the distribution results from translational energy release greater than the collision energy. The available energy is given by $E_{coll} + E_{exo} = 1.1 + 1.2 = 2.3$ eV; a substantial

fraction of the products thus appear with translational energy derived from reaction exoergicity, and $BaBr^+$ is observed to the limit of the available energy.

B. $Ba(^1P_1,^{1,3}D) + Br_2$

Laboratory angular distributions for $BaBr^+$ were measured for reaction of barium with Br_2 at collision energies of 1.1 and 1.6 eV, with a single mode ring dye laser directed to the interaction region pumping the barium ($^1S_0$-$^1P_1$) transition at 553.7 nm. The laser polarization was parallel to the relative velocity vector. Figure 4 shows both laser on and laser off angular distributions, uncorrected for the fraction of the beam excited at 1.1 eV collision energy. Shown in the same figure is the laser-induced associative ionization product $BaBr_2^+$ observed under the same conditions, kinematically constrained to appear only at angles near the center of mass. The 1.1 eV collision energy result showed roughly 20% laser-induced inhibition of $BaBr^+$ signal, largely independent of scattering angle. This is similar to results previously obtained[15] for the chlorine reaction at 0.75 eV, and the inhibition corresponds roughly to the $Ba(^1P_1)$ population at the interaction region.

However, striking changes were observed in the distributions with the increase in collision energy to 1.6 eV, shown in figure 5. Aside from the general feature of $BaBr^+$ produced by residual ground state barium in the beam (shown as dashed line), a sharp feature appeared directly behind the center of mass. Figure 6 shows laser dependent signal for the high collision energy obtained by subtracting the contributions

from the ground state Ba, and assuming the inhibition seen at the back angles corresponds to the excited state fraction of the beam. This represents the most conservative estimate of the excited state fraction. The dominant feature of course is the backscattered peak, but a substantial forward component is also apparent. The clear dip at the center of mass suggests a translational energy distribution peaking away from zero.

The associative ionization product was clearly seen at both collision energies following laser excitation, yet despite the fact that all $BaBr_2^+$ is constrained to appear clustered in the vicinity of the center of mass, the laser-dependent $BaBr^+$ at 1.6 eV was ~100 times more intense than the $BaBr_2^+$.

IV. DISCUSSION

A. $Ba + Br_2 \rightarrow BaBr^+ + Br^-$

Sections through several relevant diabatic potential energy surfaces for collinear $Ba\text{-}Br_2$ are shown in Figure 7, estimated using a semi-empirical diatomics-in-molecules method.[18,19] We have employed the diabatic representation so that the crossing points can be more easily visualized. The Br-Br internuclear distance is fixed at 2.5 Å, somewhat larger than the equilibrium distance for the neutral molecule (2.28 Å). This represents the region of the surface likely to be important for electron transfer, owing to "prestretching" of the Br-Br bond on the adiabatic surface.[20] The $Ba(^1P_1)\text{-}Br_2$ curve

actually represents three curves, two of which are degenerate in the collinear configuration. Figure 7 is intended to facilitate a qualitative discussion of the dynamics of these collisions, but it should be borne in mind that the D states and the triplet surfaces have been neglected for the sake of clarity. For the ground state reaction the first crossing of the ionic and covalent potential energy surfaces (point 1 in figure 7), occurs at ~4 Å. As mentioned above, the chemi-ion products $BaBr^+ + Br^-$ correlate to the doubly ionic Ba^{++}-Br_2^{--} surface. The chemi-ion channel thus requires access to the second crossing region (2 in Figure 7). The backscattered $BaBr^+$ distribution seen in the contour map in Figure 3 reveals the nature of the stringent requirements for gaining this access: only simultaneously collinear *and* low impact parameter collisions are able to reach this second crossing point.

An understanding of the origin of these stereochemical demands requires a consideration of the competing neutral channel, the dominant channel at these collision energies.[6] In 1972 both Bernstein and coworkers[11] and Herm et al.[12] reported results for crossed beams reaction of barium with halogen molecules. The consensus for the neutral channel was little different from that seen in the classic $K + Br_2$ reaction: long-range electron transfer results in a vertical transition to a repulsive region of the Br_2^- potential energy curve, resulting in rapid stretching of the $(Br\text{-}Br)^-$ bond with dissociation in the field of the positive ion. The experimental manifestation of this is forward scattered BaBr with little of the available energy appearing in translation. Beautiful studies of non-adiabatic pathways in the alkali-halogen reactions by Los and Kleyn[9,10,20] provide a deep experimental understanding of the "harpoon mechanism"

outlined above. Following initial electron transfer, the rapidly changing bond distance in the vibrationally excited anion results in a corresponding change in the electron affinity, or viewed from a different perspective, the location of the crossing seam. The probability of electron transfer on exit may thus be very different from that on approach. In the case of high energy collisions of $Cs\text{-}O_2$, this phenomenon gave rise to oscillations in the angular distributions of Cs^+ corresponding to the vibrational period of O_2^-. The important aspect for the present discussion is that rapid stretching of the $(Br\text{-}Br)^-$ bond accompanies electron transfer. Immediately on reaching the singly ionic surface (1 in Figure 7), the reactive system rapidly escapes into the exit valley leading to neutral BaBr and Br. For collinear, low impact parameter trajectories this escape, leaving the Br atom as spectator, is simply not possible. Instead, transfer of the second electron takes place when the nascent bromine atom and the nascent BaBr are pushed together with their respective linear momentum. The result is a close collision forming a tightly packed $Ba^{2+}Br^-Br^-$ collinear intermediate. Because of the repulsion between the negatively charged bromine atoms, the backscattered $BaBr^+$ appears with a substantial fraction of the available energy released into translation. The magnitude of the chemi-ion cross section (0.6 $Å^2$)[13] is also consistent with the limited contribution of these sterically constrained collisions relative to the overall harpooning cross section (~50 $Å^2$).

Additional evidence for this interpretation is provided by the results for electronically excited barium. The excited state composition of the barium beam is not precisely known owing to the presence of metastable D states populated by

radiative decay from the $^1P_1$. Evidence obtained by exciting upstream of the interaction region in studies with Cl_2 indicated that the D states were less effective at inhibiting the chemi-ion cross section than the $^1P_1$.[15] We will focus our discussion on $Ba(^1P_1)$, though these arguments are consistent with what is seen with the D states alone. For $Ba(^1P_1)$, laser excitation adds an additional 2.2 eV to the energy available to the system. Moreover, the first crossing is moved out a considerable distance: from 4 Å to 12 Å (indicated at 1* in figure 7). The implications of this in the model outlined above are apparent: the distance between the first and second crossing points has changed from ~1Å to ~9Å. Using the initial relative velocity we can estimate the time between crossings for collinear approach: about 60 femtoseconds for the ground state reaction yet 540 femtoseconds for the excited state. The vibrational period of the excited Br_2^- is ~310 femtoseconds.[10] From the excited surface, even for very nearly collinear collisions, the remaining bromine atom has ample time to escape. Moreover, even if a secondary collinear encounter between Br and highly vibrationally excited BaBr were to take place, the chances of the three atoms achieving the tightly packed configuration corresponding to the region of the second crossing may be very limited. This probably results in redirection of flux into neutral products, yet this may represent only a minimal increase in the overall neutral cross section.

B. $Ba(^1P_1,^{1,3}D_J) + Br_2$

Because the associative ionization product $BaBr_2^+$ recoils from an electron, momentum conservation requires that it appear in the vicinity of the center of mass of the system. Consequently, information about its role in the dynamics of these collisions must be sought in the relative magnitude and energy and laser dependencies of the cross section, rather than in the angular or translational energy distributions. It is weakly observed from the ground state at 1.6 eV, but is greatly enhanced on laser excitation, then appearing clearly at both 1.1 and 1.6 eV. No attempt was made to discern the relative contribution of the barium P or D states to the laser enhancement of $BaBr_2^+$. The associative ionization may result from ejection of an electron at the classical turning point of the transient $Ba\text{-}Br_2$ collision if a vertical transition to a stable product ion is possible. Such a transition requires that the transient $Ba\text{-}Br_2$ complex achieve a geometry close to that of the product ion in order for the reaction to be energetically feasible. It is clear from the discussion above that the vast majority of collisions do not gain access to the deep $Br^-Ba^{++}Br^-$ well. It is not accessible in the collinear space we have considered so far. Nevertheless, there will be C_{2v} collisions and they are the most likely to achieve a geometry close to that of $BaBr_2^+$, probably after overcoming a potential energy barrier. Electron transfer at the outer crossing is not favored by A_1 and B_1 configurations in C_{2v} geometry, so a close collision from the covalent surface is quite plausible. The additional photon energy may simply serve to bring the total energy over the ionization threshold for a greater number of collisions, allowing the system to reach the region of the potential energy surface where electron ejection may occur.

The source of the laser enhanced $BaBr^+$ observed at 1.6 eV may now be considered. The signal shown in Figure 6 displayed a sharp threshold behavior: it was not evident at all at collision energies much below 1.5 eV. As discussed above, one of the important consequences of electronic excitation of the barium atom is to move the first crossing to very large Ba-Br distance. Even for near collinear collisions the second Br atom may behave as a spectator in the initial interaction, but at this higher collision energy it may not escape prior to a second collision with the newly formed, highly vibrationally excited BaBr. If one assumes no initial transfer of momentum from the second Br atom to BaBr, one obtains the BaBr center of mass recoil velocity in the "spectator limit", and this is shown as the spectator stripping circle in Figure 6. A secondary BaBr-Br collision would be characterized by this same velocity, so the circle represents the elastic maximum for a secondary encounter in the spectator limit. All of the laser dependent $BaBr^+$ falls well within this maximum. The tendency to backscattering is a consequence of the fact that these secondary collisions can only result from near collinear trajectories. The low translational energy release may thus be understood to result naturally from conservation of linear momentum in both collisional encounters. Yet the final translational energy appears to peak sharply at approximately half of the velocity dictated in the spectator limit. This reveals the deviation from the limiting case: there may be substantial repulsion between the bromine atoms following initial electron transfer, and from the final translational energy we may estimate its magnitude. A simple calculation assuming an elastic secondary collision suggests initial Br-Br relative velocity of 900 m/s at the point of

the second collision. This accounts for the low translational energy release, and suggests a dynamic rather than energetic explanation for the sharp threshold. The features of a secondary collision are very sensitive to the initial vibrational energy of the halogen molecular ion and the phase of this vibration relative to the approaching barium atom. Very different behavior would be expected for Cl_2, and indeed no analogous laser dependent signal was observed for $BaCl^+$ in previous studies at several collision energies from 0.75 to 3.0 eV.

We have not addressed the question of the final product states: both $BaBr^+ + Br^-$ and $BaBr^+ + Br + e^-$ are possible product channels, the latter approximately thermoneutral for $Ba(^1P_1) + Br_2$. The $BaBr^+$ might result from autoionization of highly vibrationally excited BaBr resulting from the second collision. Alternatively, favorable second collisions may achieve the tightly packed geometry at the region of an inner crossing to the doubly ionic $BaBr^+ + Br^-$ potential energy surface. Both product channels appear plausible, and negative ion detection would be useful to discriminate between them.

V. CONCLUSION

The ground state, neutral products which dominate the reaction of barium with halogen molecules reveal little of the dynamical richness that is present. By studying ions produced in these reactions at modest collision energies, the dynamics in this prototypical divalent system may be drawn out. The chemi-ion products $BaBr^+$ and

Br^- were found to result from near-zero impact parameter, collinear collisions. These severe stereochemical constraints arise out of competition with the dominant neutral channel. At 1.1 eV, the reaction was inhibited from the $Ba(^1P_1)$-Br_2 excited surface, again owing to the dynamic competition with the neutral channel. At 1.6 eV a laser dependent $BaBr^+$ signal appeared, probably also the result of collinear collisions, but derived from the neutral channel and involving a secondary encounter. A laser dependent associative ionization channel was observed at both collision energies studied, more than 100 fold weaker than the chemi-ion reaction. This associative ionization reaction probably results from ejection of an electron at the classical turning point of a $BaBr_2$ collision for those C_{2v} collisions which gain access to a region of the neutral potential energy surface for which the nuclear geometry resembles the product ion.

Acknowledgement

This work was supported by the Director, Office of Energy Research, Office of Basic Energy Sciences, Chemical Sciences Division, of the U. S. Department of Energy under contract No. DE-AC03-76SF00098. A.G.S. thanks the NSF for a graduate fellowship.

REFERENCES

1. Michael Menzinger, The M + X_2 Reactions: A Case Study, in **Gas Phase Chemiluminescence and Chemi-Ionization**, A. Fontijn, ed., Elsevier Science Publishers, B.V., 1985, pp.25-66, and references therein.
2. C. D. Jonah and R. N. Zare, Chem. Phys. Lett. **9**, 65 (1971).
3. D. J. Wren and M. Menzinger, Chem. Phys. Lett. **27**, 572 (1974).
4. C. T. Rettner and R. N. Zare, J. Chem. Phys. **77**, 2416 (1982).
5. H. F. Davis, A. G. Suits, H. Hou and Y. T. Lee, Ber. Bunsenges. Phys. Chem., in press.
6. M. Menzinger, J. Phys. Chem. **94**, 1899 (1990).
7. D. R. Herschbach, Adv. Chem. Phys. **10**, 319 (1966).
8. R. Grice, Adv. Chem. Phys. **30**, 247 (1975).
9. M. M. Hubers, A. W. Kleyn and J. Los, Chem. Phys. **17**, 303 (1976).
10. J. Los and A. W. Kleyn, Ion Pair Formation, in **Alkali Halide Vapors**, P. Davidovits and D. L. McFadden, eds., Academic Press, New York, (1979) pp. 275-331.
11. J. A. Haberman, K. G. Anlauf, R. B. Bernstein and F. J. Van Itallie, Chem. Phys. Lett., **16**, 442 (1972).
12. Shen-Maw Lin, Charles A. Mims, and Ronald R. Herm, J. Chem. Phys. **58**, 327 (1973).
13. G. J. Diebold, F. Engelke, H. U. Lee, J. C. Whitehead, and R. N. Zare, Chem. Phys. **30**, 265 (1977).

14. R. H. Burton, J. H. Brophy, C. A. Mims and J. Ross, J. Chem. Phys. **73**, 1612 (1980).

15. A. G. Suits, H. Hou and Y. T. Lee, J. Phys. Chem. **94**, 5672 (1990).

16. H. F. Davis, M. H. Covinsky, A. G. Suits and Y. T. Lee, to be published.

17. Y. T. Lee, J. D. McDonald, P. R. LeBreton and D. R. Herschbach, Rev. Sci. Instrum. **40**, 1402 (1969).

18. F. O. Ellison, J. Am. Chem. Soc., **85**, 3540 (1963).

19. E. M. Garfield, E. A. Gislason and N. H. Sabelli, J. Chem. Phys. **82** 3179 (1985).

20. J. A. Aten and J. Los, Chem. Phys. **25**, 47 (1977).

Figure Captions

Figure 1. Schematic view of crossed beams apparatus at interaction region showing modifications for detection of ions.

Figure 2. Translational energy scans for $BaBr^+$ from reaction of ground state Ba with Br_2 at a collision energy of 1.1 eV, shown with fits obtained by forward convolution as described in text. Laboratory scattering angles are shown, measured with respect to the Ba beam.

Figure 3. $BaBr^+$ flux-velocity contour map obtained from the fit shown in Figure 2 for $Ba(^1S_0) + Br_2 \rightarrow BaBr^+ + Br^-$ at 1.1 eV collision energy, shown superimposed on the nominal Newton diagram.

Figure 4. Laboratory angular distribution of $BaBr^+$ from reaction of Ba with Br_2 for ground state Ba (circles) and with a laser saturating the $Ba(^1S_0\text{-}^1P_1)$ transition at the interaction region (squares) at 1.1 eV collision energy. Also shown is the associative ionization product $BaBr_2^+$ (triangles) for the laser-on case, enhanced 25-fold.

Figure 5. Laboratory angular distribution of $BaBr^+$ from reaction of Ba with Br_2 for ground state Ba (circles) and with a laser saturating the $Ba(^1S_0\text{-}^1P_1)$ transition at the interaction region (squares) at 1.6 eV collision energy. Dotted line shows estimated contribution of ground state reaction to the laser excited signal.

Figure 6. Laboratory angular distribution of laser-dependent $BaBr^+$ (circles) and $BaBr_2^+$ (triangles) obtained from the data shown in Figure 5. The ground state contribution was subtracted as described in the text. The nominal Newton diagram is shown with the circle corresponding to the BaBr recoil velocity in the spectator stripping limit. Laboratory angles 20 and 60 degrees are indicated by dotted lines. The associative ionization product $BaBr_2^+$ is shown enhanced 25 fold.

Figure 7. Sections through several diabatic potential energy surfaces for collinear $Ba\text{-}Br_2$ obtained as described in text.

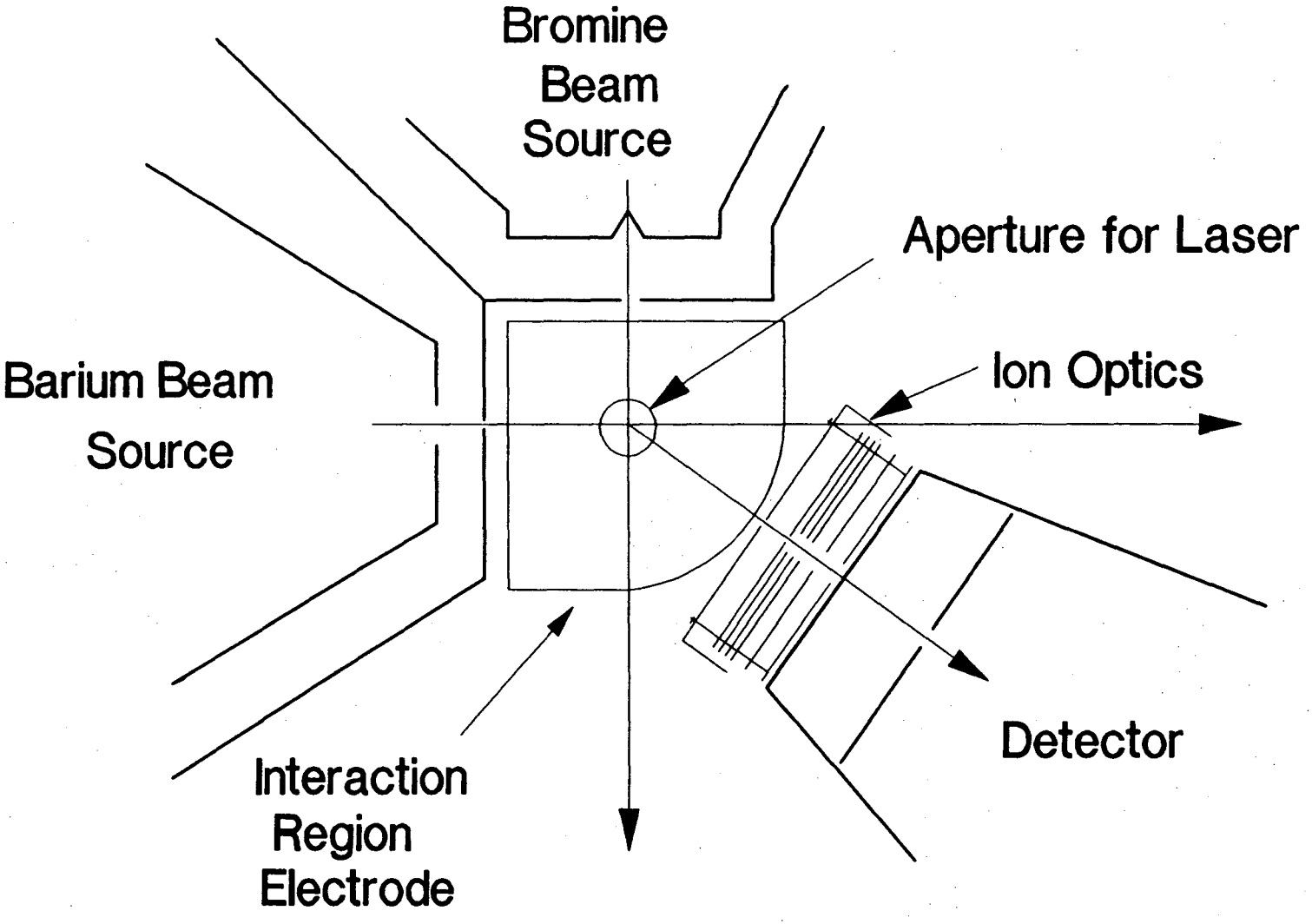
Bromine
Beam
Source
Aperture for Laser
Barium Beam
Source
Ion Optics
Detector
Interaction
Region
Electrode

Fig. 1

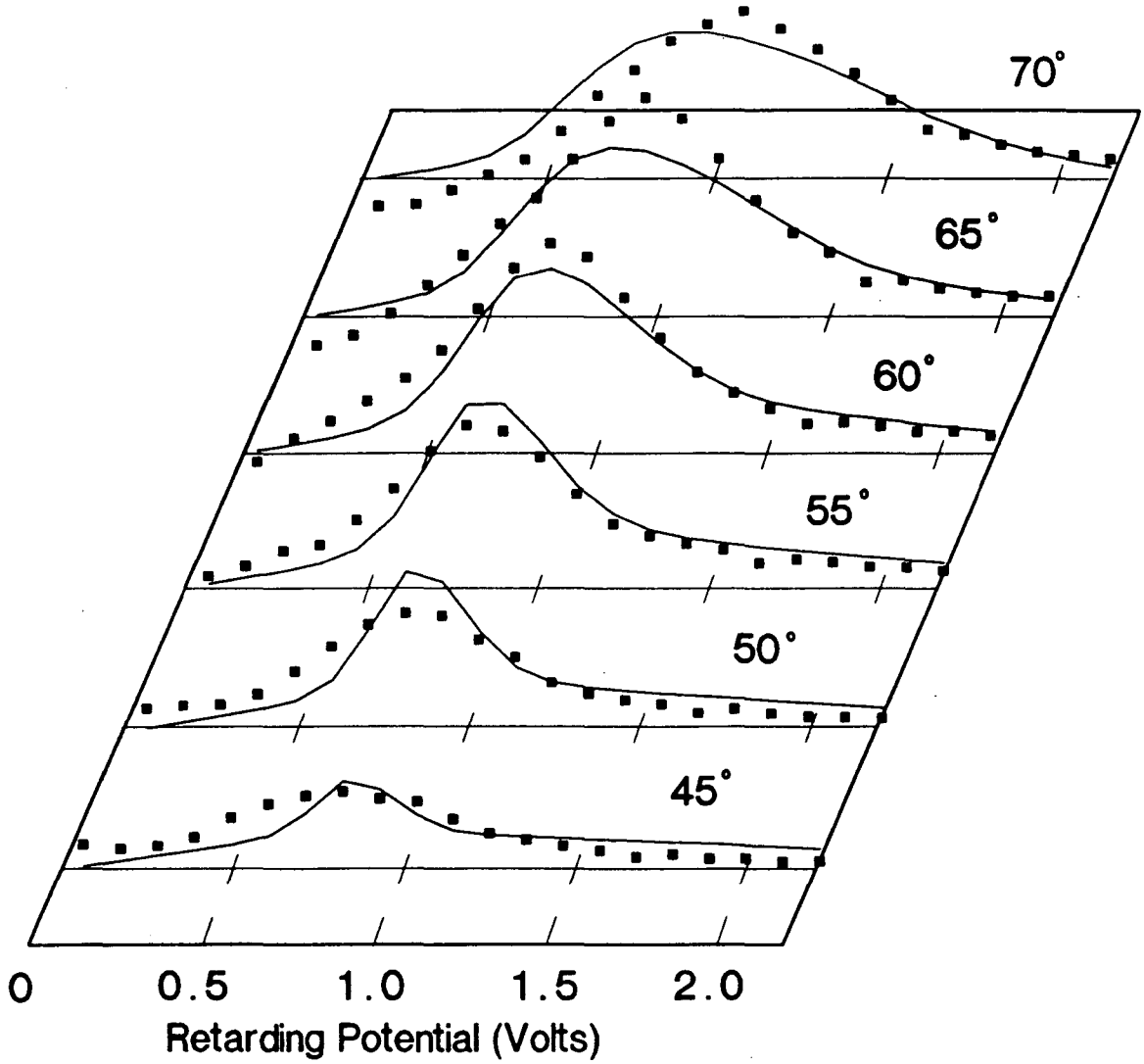

Fig. 2

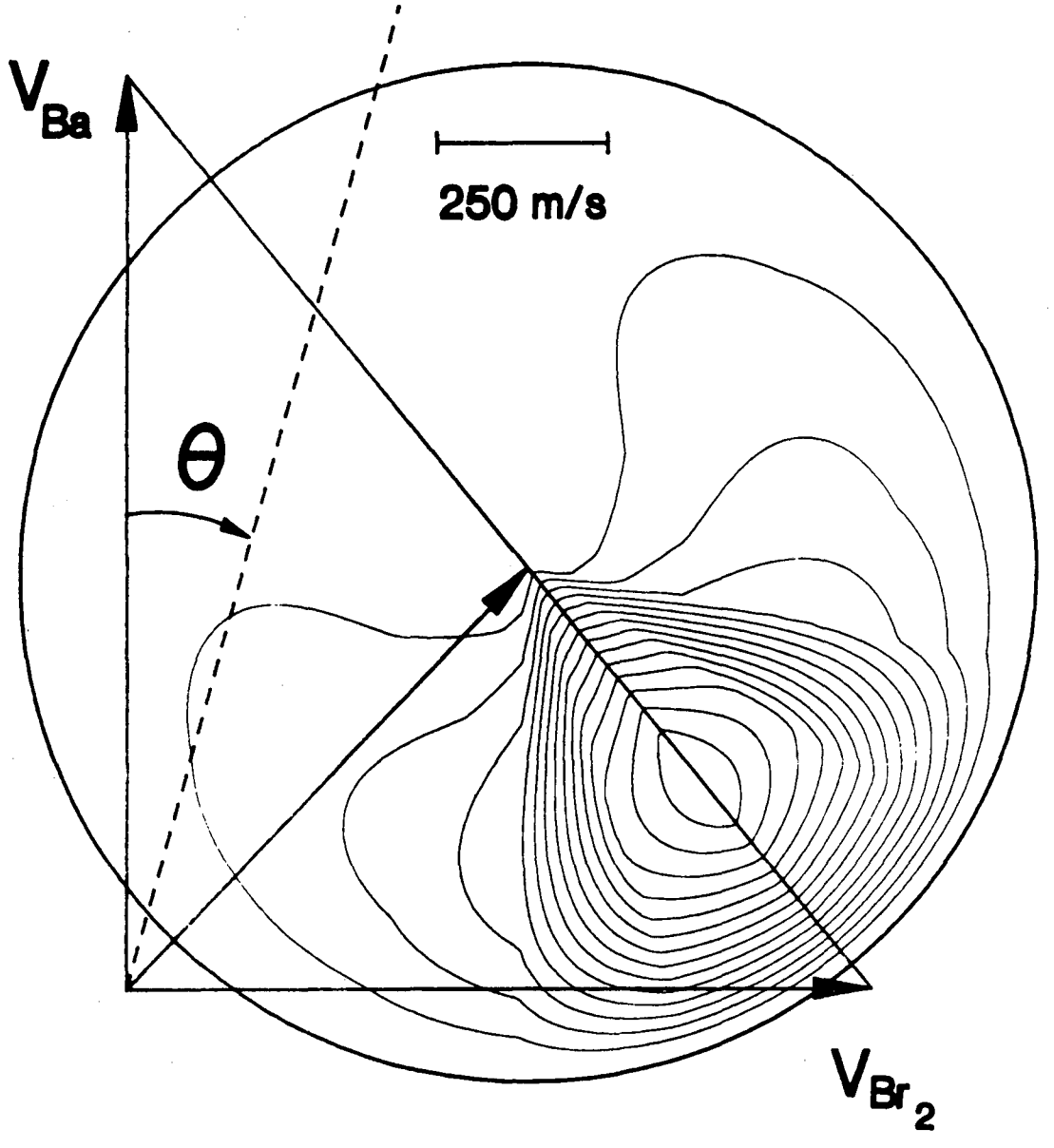

Fig. 3

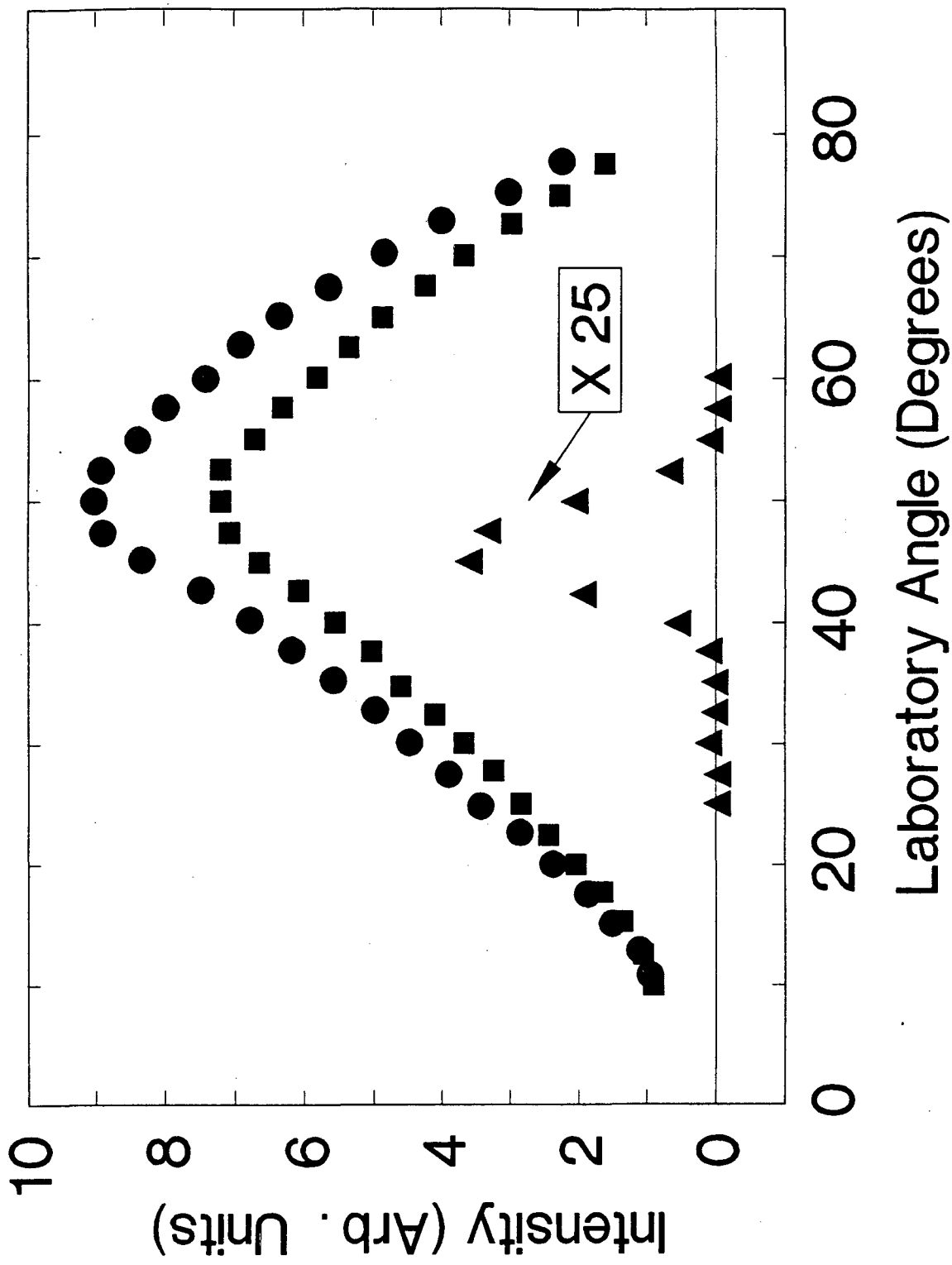
Intensity (Arb. Units)
0
2
4
6
8
10
0
20
40
60
80
Laboratory Angle (Degrees)
X 25

Fig. 4

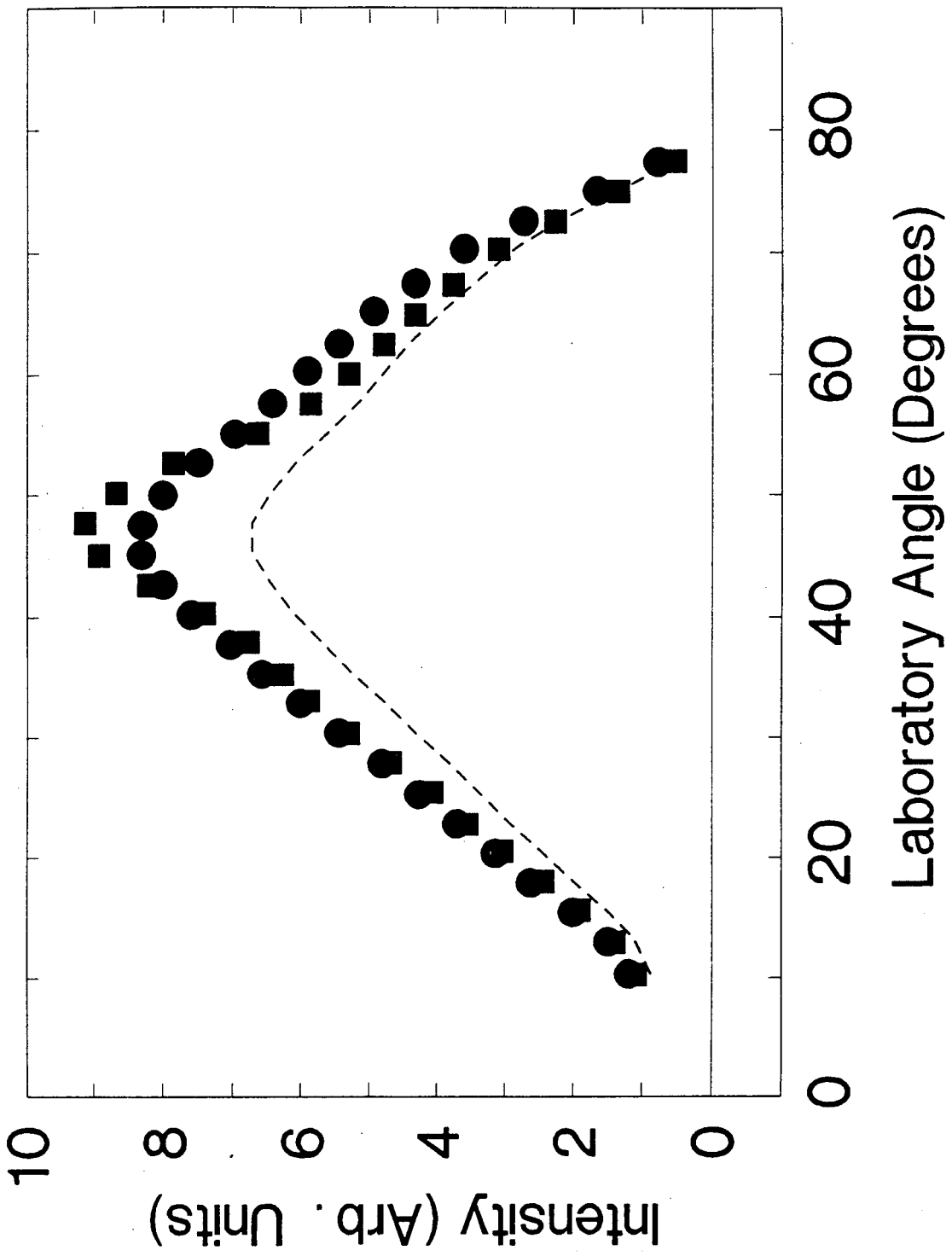
Intensity (Arb. Units)
10
8
6
4
2
0
0
20
40
60
80
Laboratory Angle (Degrees)

Fig. 5

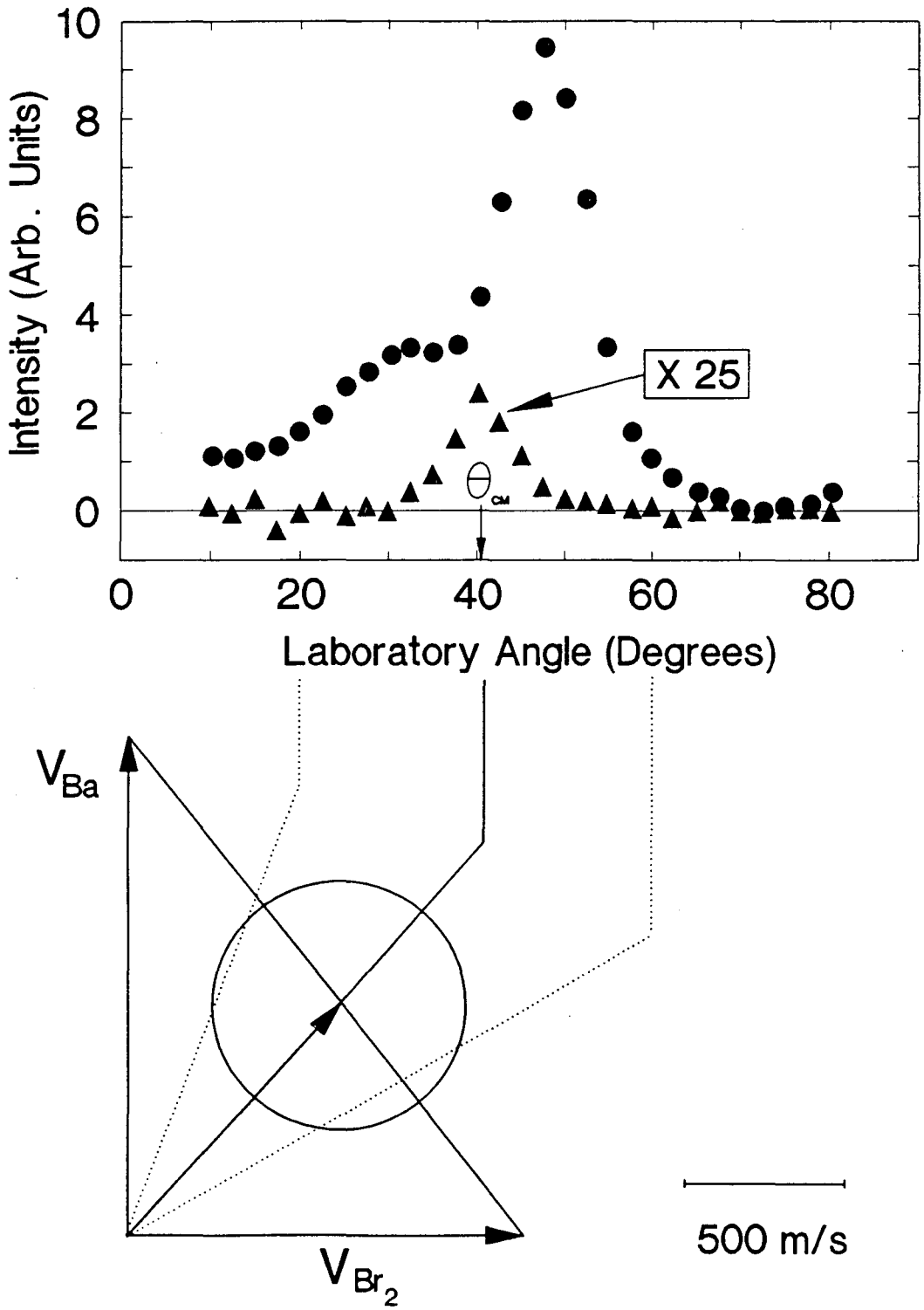
10
8
6
4
2
0
Intensity (Arb. Units)
X 25
Θ_{CM}
0
20
40
60
80
Laboratory Angle (Degrees)
V_{Ba}
V_{Br_2}
500 m/s

Fig. 6

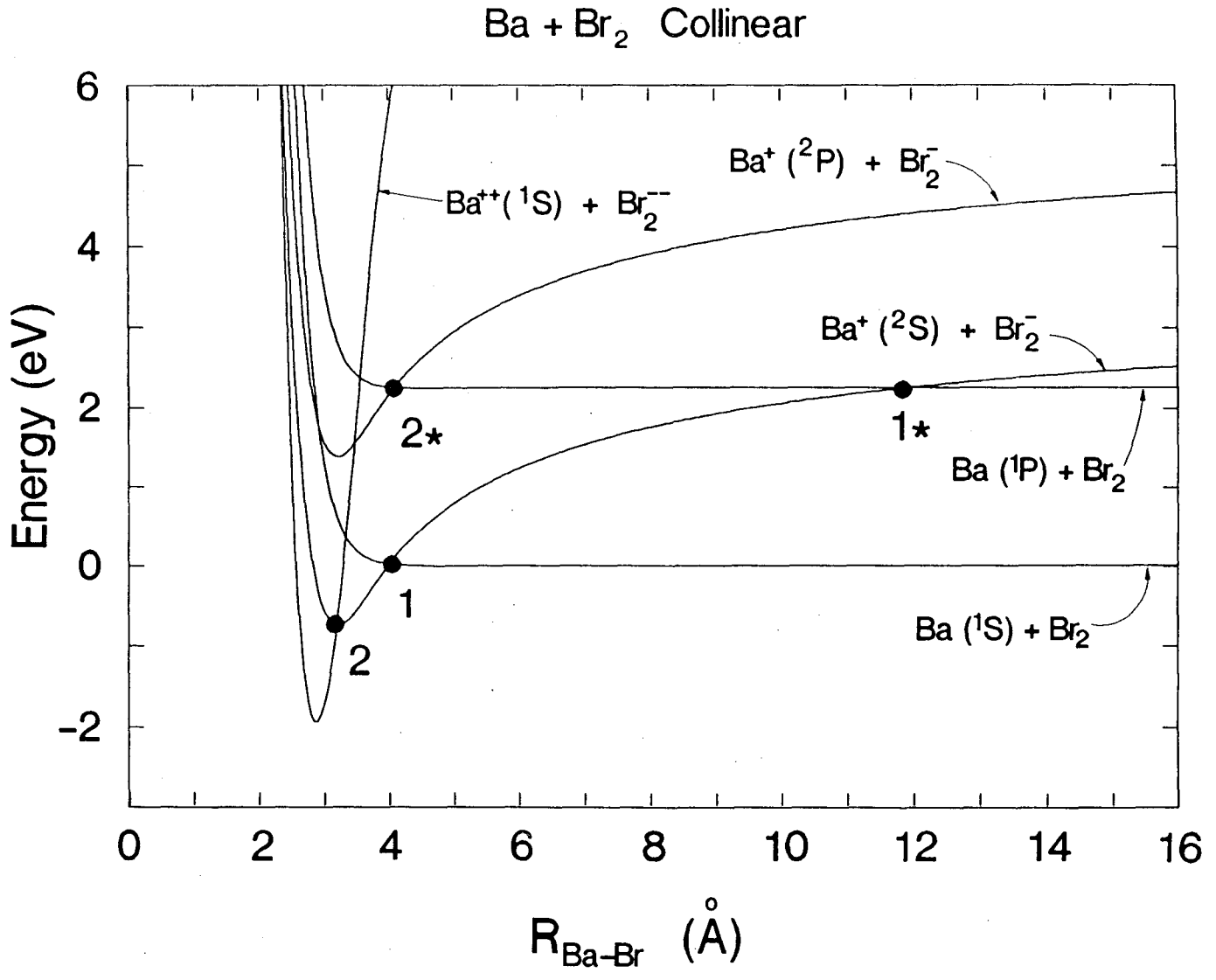
Ba + Br2 Collinear
Energy (eV)
6
4
2
0
-2
0
2
4
6
8
10
12
14
16
R Ba-Br (Å)
Ba++(1S) + Br2---
Ba+ (2P) + Br2-
Ba+ (2S) + Br2-
Ba (1P) + Br2
Ba (1S) + Br2
2*
1*
1
2

Fig. 7

LAWRENCE BERKELEY LABORATORY
UNIVERSITY OF CALIFORNIA
INFORMATION RESOURCES DEPARTMENT
BERKELEY, CALIFORNIA 94720